Inorganic Chemistry
Article

Inorg. Chem. **2010**, *49*, 11541–11549 **11541**
DOI: 10.1021/ic101970j

Defective Dicubane-like Tetranuclear Nickel(II) Cyanate and Azide Nanoscale Magnets

Zurine Serna,[†] Noelia De la Pinta,[†] M. Karmele Urtiaga,[‡] Luis Lezama,[†] Gotzon Madariaga,[§] J. Modesto Clemente-Juan,[⊥] Eugenio Coronado,[⊥] and Roberto Cortés*,[†]

[†]*Departamento de Química Inorgánica,* [‡]*Departamento de Mineralogía y Petrología, and*
[§]*Departamento de Física de la Materia Condensada, Universidad del País Vasco, Apartado 644, 48080 Bilbao,*
Spain, and [⊥]*Instituto de Ciencia Molecular, Edificios Institutos de Paterna, Universidad de Valencia,*
C/Catedrático Jose Beltrán, 2, 46980 Paterna-Valencia, Spain

Received September 27, 2010

Four tetrameric nickel(II) pseudohalide complexes have been synthesized and structurally, spectroscopically, and magnetically characterized. Compounds **1**−**3** are isostructural and exhibit the general formula $[Ni_2(dpk \cdot OH)(dpk \cdot CH_3O)(L)(H_2O)]_2A_2 \cdot 2H_2O$, where dpk = di-2-pyridylketone; L = N_3^-, and A = ClO_4^- for **1**, L = NCO^- and A = ClO_4^- for **2**, and L = NCO^- and A = NO_3^- for **3**. The formula for **4** is $[Ni_4(dpk \cdot OH)_3 (dpk \cdot CH_3O)_2(NCO)](BF_4)_2 \cdot 3H_2O$. The ligands $dpk \cdot OH^-$ and $dpk \cdot CH_3O^-$ result from solvolysis and ulterior deprotonation of dpk in water and methanol, respectively. The four tetramers exhibit a dicubane-like core with two missing vertexes where the Ni^{II} ions are connected through end-on pseudohalide and oxo bridges. Magnetic measurements showed that compounds **1**−**4** are ferromagnetic. The values of the exchange constants were determined by means of a theoretical model based on three different types of coupling. Thus, the calculated J values ($J_1 = J_2$, J_3, and D) were 5.6, 11.8, and 5.6 cm^{-1} for **1**, 5.5, 12.0, and 5.6 cm^{-1} for **2**, 6.3, 4.9, and 6.2 cm^{-1} for **3**, and (J_1, J_2, J_3, and D) 6.9, 7.0, 15.2, and 4.8 cm^{-1} for **4**.

Introduction

The preparation of molecule-based magnets has been the subject of many works in coordination chemistry.[1] From this research field, the way to deal with this challenge consists of the synthesis of single molecules exhibiting electronic ground states with a large number of unpaired electrons because it has been discovered that a fairly large ground state S value is one of the necessary requirements for molecules to be able to exhibit the behavior of a single-molecule magnet.[2] In this context, enhancing both the nuclearity and the anisotropy of the clusters has been one of the main objectives because they are directly related to the nature and extension of the magnetic coupling. Besides, ferro- or ferrimagnetic interactions in the molecules are required to obtain the high-spin ground state. Many of the clusters for nanomagnets characterized to date exhibiting high nuclearity involve intermetallic bridges through O atoms. However, in most of the cases, these magnetic pathways provide modest values of the exchange coupling or even antiferromagnetism. In this case, the selection of a metallic cation enhancing the cluster anisotropy would be very convenient, and Ni^{II} represents a good choice because this metallic cation shows an important zero-field splitting.[3]

An efficient way for the generation of ferromagnetic intervactions between metallic centers concerns the use of pseudohalide ligands. Among these, it is well-known that the azide one in its 1,1-fashion propagates ferromagetism.[4a−s] In

---

*To whom correspondence should be addressed. E-mail: roberto.cortes@ehu.es.

[1] (a) Ferlay, S.; Mallah, T.; Ouahès, R.; Veillet, P.; Verdaguer, M. *Inorg. Chem.* **1999**, *38*, 229–234. (b) Tangoulis, V.; Raptopoulou, C. P.; Terzis, A.; Bakalbassis, E. G.; Diamantopoulou, E.; Perlepes, S. P. *Inorg. Chem.* **1998**, *37*, 3142–3153. (c) Aromí, G.; Claude, J.-P.; Knapp, M. J.; Huffman, J. C.; Hendrickson, D. N.; Christou, G. *J. Am. Chem. Soc.* **1998**, *120*, 2977–2978. (d) Aromí, G.; Aubin, S. M. J.; Bolcar, M. A.; Christou, G.; Eppley, H. J.; Folting, K.; Hendrickson, D. N.; Huffmann, J. C.; Squire, R. C.; Tsai, H.-L.; Wang, S.; Wemple, M. W. *Polyhedron* **1998**, *17*, 3005–3020. (e) Bolcar, M. A.; Aubin, S. M. J.; Folting, K.; Hendrickson, D. N.; Christou, G. *Chem. Commun.* **1997**, 1485–1486. (f) Caneschi, A.; Gatteschi, D.; Sessoli, R. *J. Chem. Soc., Dalton Trans.* **1997**, 3963. (g) Goldber, D. P.; Caneschi, A.; Delfs, C. D.; Sessoli, R.; Lippard, S. J. *J. Am. Chem. Soc.* **1995**, *117*, 5789–5800. (h) Powell, A. K.; Heath, S. L.; Gatteschi, D.; Pardi, L.; Sessoli, R.; Spina, G.; Giallo, F. D.; Pieralli, F. *J. Am. Chem. Soc.* **1995**, *117*, 2491–2502. (i) Sessoli, R.; Tsai, H.-L.; Schake, A. R.; Wang, S.; Vincent, J. B.; Folting, K.; Gatteschi, D.; Christou, G.; Hendrickson, D. N. *J. Am. Chem. Soc.* **1993**, *115*, 1804–1816. (j) Aubin, S. M. J.; Wemple, M. W.; Adams, D. M.; Tsai, H.-L.; Christou, G.; Hendrickson, D. N. *J. Am. Chem. Soc.* **1996**, *118*, 7746–7754. (k) Coronado, E.; Galán-Mascarós, J. R.; Gomez-García, C. J.; Martinez-Agudo, J. M. *Inorg. Chem.* **2001**, *40*, 113–120. (l) Ren, X.; Meng, Q.; Song, Y.; Lu, C.; Hu, C. *Inorg. Chem.* **2002**, *41*, 5686–5692. (m) Miller, J. S.; Epstein, A. J. *Angew. Chem., Int. Ed.* **2003**, *33*, 385–415. (n) Kashiwagi, T.; Ohkoshi, S.-I.; Seino, H.; Mizobe, Y.; Hashimoto, K. *J. Am. Chem. Soc.* **2004**, *126*, 5024–5025. (o) Sorai, M.; Nakano, M.; Miyazaki, Y. *Chem. Rev.* **2006**, *106*, 976–1031.

[2] (a) Mataga, N. *Theor. Chim. Acta* **1968**, *10*, 378–382. (b) Gatteschi, D.; Sessoli, R.; Cornia, A. *Chem. Commun.* **2000**, 725–727. (c) Yoo, J.; Brechin, E. K.; Yamaguchi, A.; Nakano, M.; Huffman, J. C.; Maniero, A. L.; Brunel, L.-C.; Awaga, A.; Ishimoto, H.; Christou, G.; Hendrickson, D. N. *Inorg. Chem.* **2000**, *39*, 3615–3623 and references cited therein.

the same way, an 1,1-N-cyanate ligand, which is more unusual, is also able to give this kind of interaction.[4t−z] With the aim of facilitating the formation of nickel(II) pseudohalide clusters, a versatile organic ligand should also be used. To this respect, di-2-pyridylketone (dpk) seems to be an excellent candidate because it exhibits three potential donors, being able to chelate in bidentate (N,N or N,O) or tridentate (N,O,N) modes. Moreover, dpk has been observed occasionally to undergo solvolysis, resulting in a derivative product that can coordinate either as a neutral ligand (dpk·ROH) or as an anionic ligand (dpk·RO$^-$) (Scheme 1).[5]

Taking into account these considerations, we have been working on the M^{II}dpk (M = Mn, Co, Ni, and Cu) system using azide, cyanate, and thiocyanate as pseudohalides.[6] Our results in this work concern the magnetostructural characterization of four dicubane-like tetrameric clusters. Three of them are isostructural and exhibit the general formula [Ni$_2$(dpk·OH)(dpk·CH$_3$O)(L)(H$_2$O)]$_2$A$_2$·2H$_2$O, where L = N$_3^-$ and A = ClO$_4^-$ for **1**, L = NCO$^-$ and A = ClO$_4^-$ for **2**, and L = NCO$^-$ and A = NO$_3^-$ for **3**. Compound **4** exhibits the formula [Ni$_4$(dpk·OH)$_3$(dpk·CH$_3$O)$_2$(NCO)](BF$_4$)$_2$·3H$_2$O. The groups dpk·OH$^-$ and dpk·CH$_3$O$^-$ result from solvolysis and ulterior deprotonation of dpk in water and methanol, respectively. This paper also deals with the theoretical treatment of the magnetic data for **1**−**4**, which have been observed to be ferromagnetic. Some of the results herein reported concerning compound **1** have been previously published in a preliminary communication.[6b]

Scheme 1. Different Modes of the dpk Ligand

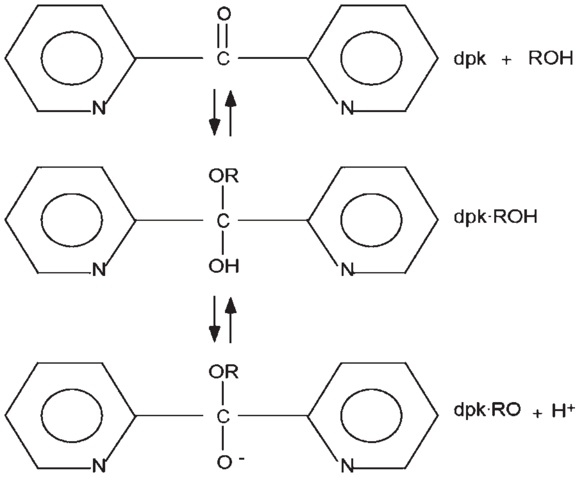

---

(3) (a) Martinez-Lillo, J.; Armentano, D.; De Munno, G.; Wernsdorfer, W.; Clemente-Juan, J. M.; Krzystek, J.; Lloret, F.; Julve, M.; Faus, J. *Inorg. Chem.* **2009**, *48*, 3027–3038. (b) Clemente-Juan, J. M.; Coronado, E.; Galán-Mascarós, J. R.; Gómez-García, C. J. *Inorg. Chem.* **1999**, *38*, 55–63. (c) Faus, J.; Lloret, F.; Julve, M.; Clemente-Juan, J. M.; Muñoz, M. C.; Solans, X.; Font-Bardía, M. *Angew. Chem., Int. Ed.* **1996**, *35*, 1485–1487. (d) Salah El Fallah, M.; Rentschler, E.; Caneschi, A.; Sessoli, R.; Gatteschi, D. *Inorg. Chem.* **1996**, *35*, 3723–3724. (e) Blake, A. J.; Brechin, E. K.; Codron, A.; Gould, R. O.; Grant, C. M.; Parsons, S.; Rawson, J. M.; Winpenny, R. E. P. *J. Chem. Soc., Chem. Commun.***1995**, 1983–1985. (f) Bakalbassis, E. G.; Diamantopoulou, E.; Perlepes, S. P.; Raptopoulou, C. P.; Tangoulis, V.; Terzis, A.; Zafiropoulos, T. F. *J. Chem. Soc., Chem. Commun.* **1995**, 1347–1348. (g) Halcrow, M. A.; Sun, J.-S.; Huffman, J. C.; Christou, G. *Inorg. Chem.* **1995**, *34*, 4167–4177. (h) Halcrow, M. A.; Huffman, J. C.; Christou, G. *Angew. Chem., Int. Ed.* **1995**, *34*, 889–891. (i) Ribas, J.; Monfort, M.; Costa, R.; Solans, X. *Inorg. Chem.* **1993**, *32*, 695–699. (j) Wu, D.-Y.; Huang, W.; Hua, W.-H.; Song, Y.; Duan, C.-Y.; Li, S.-H.; Meng, Q.-J. *Dalton Trans.* **2007**, 1838–1845.

(4) For azide, see: (a) Commarmond, J.; Plumeré, P.; Lehn, J. M.; Agnus, Y.; Louis, R.; Weiss, R.; Kahn, O.; Morgenstern-Badarau, I. *J. Am. Chem. Soc.* **1982**, *104*, 6330–6340. (b) Cortés, R.; Lezama, L.; Mautner, F. A.; Rojo, T. *Molecule Based Magnetic Materials*; American Chemical Society: Washington, DC, 1996; Chapter 12, pp 187−200. (c) Ruiz, E.; Cano, J.; Alvarez, S.; Alemany, P. *J. Am. Chem. Soc.* **1998**, *120*, 11122–11129. (d) Liu, C.-M.; Yu, Z.; Xiong, R.-G.; Liu, K.; You, X.-Z. *Inorg. Chem. Commun.* **1999**, *2*, 31. (e) Ribas, J.; Escuer, A.; Monfort, M.; Vicente, R.; Cortés, R.; Lezama, L.; Rojo, T. *Coord. Chem. Rev.* **1999**, *195*, 1027–1068 and references cited therein. (f) Abu-Youssef, M. A. M.; Drillon, M.; Escuer, A.; Goher, M. A. S.; Mautner, F.; Vicente, R. *Inorg. Chem.* **2000**, *39*, 5022–5027. (g) Monfort, M.; Resino, I.; Ribas, J.; Stoeckli-Evans, H. *Angew. Chem., Int. Ed.* **2000**, *39*, 191–193. (h) Serna, Z.; Lezama, L.; Urtiaga, M. K.; Arriortua, M. I.; Barandika, M. G.; Cortes, R.; Rojo, T. *Angew. Chem., Int. Ed.* **2000**, *39*, 344–347. (i) Karmakar, T. K.; Kandra, S. K.; Ribas, J.; Mostafa, G.; Lu, T. H.; Gosh, B. K. *Chem. Commun.* **2002**, 2364–2365. (j) Demeshko, S.; Leibeling, G.; Maringgele, W.; Meyder, F.; Mennerich, C.; Klauss, H.-H.; Pritzkow, H. *Inorg. Chem.* **2005**, *44*, 519–528. (k) Sarkar, S.; Datta, A.; Mondal, A.; Chopra, D.; Ribas, J.; Rajak, K. K.; Sairam, S. M.; Pati, S. K. *J. Phys. Chem. B* **2006**, *110*, 12–15. (l) Escuer, A.; Aromí, G. *Eur. J. Inorg. Chem.* **2006**, 4721–4736 and references cited therein. (m) Mandal, D.; Bertolasi, V.; Ribas-Ariño, J.; Aromí, G.; Ray, D. *Inorg. Chem.* **2008**, *47*, 3465–3467. (n) Zhao, J.-P.; Hu, B.-W.; Sañudo, E. C.; Yang, Q.; Zeng, Y.-F.; Bu, X.-H. *Inorg. Chem.* **2009**, *48*, 2482–2489. (o) Yoon, J. H.; Ryu, D. W.; Kim, H. C.; Yoon, S. W.; Suh, B. J.; Hong, C. S. *Chem.—Eur. J.* **2009**, *15*, 3661. (p) Tandon, S. S.; Bunge, S. D.; Rakosi, R.; Xu, Z.; Thompson, L. K. *J. Chem. Soc., Dalton Trans.* **2009**, 6536–6551. (q) Stamatatos, T. C.; Abboud, K. A.; Wernsdorfer, W.; Christou, G. *Inorg. Chem.* **2009**, *48*, 807–809. (r) Zeng, M.-H.; Zhou, Y.-L.; Zhang, W.-X.; Du, M.; Sun, H.-L. *Cryst. Growth Des.* **2010**, *10*, 20–24. (s) Hu, B.-W.; Zhao, J.-P.; Tao, J.; Sun, X.-J.; Yang, Q.; Zhang, X.-F.; Bu, X.-H. *Cryst. Growth Des.* **2010**, *10*, 2829–2831. For cyanate, see: (t) Bursmeister, J. L. *Coord. Chem. Rev.* **1968**, *3*, 225–245. (u) Norbury, A. H. *Adv. Inorg. Chem. Radiochem.* **1975**, *17*, 232–236. (v) Kohout, J.; Havastijova, M.; Gazo, J. *Coord. Chem. Rev.* **1987**, *27*, 141–172. (w) Arriortua, M. I.; Cortés, R.; Mesa, J. L.; Lezama, L.; Rojo, T.; Villeneuve, G. *Transition Met. Chem.* **1988**, *13*, 371–375. (x) Boudalis, A. K.; Clemente-Juan, J.-M.; Dahan, F.; Tuchagues, J. P. *Inorg. Chem.* **2004**, *43*, 1574–1586. (y) Dey, S. K.; Mondal, N.; Salah El Fallah, M.; Vicente, R.; Escuer, A.; Solans, X.; Font-Bardía, M.; Matsushita, T.; Gramlich, V.; Mitra, S. *Inorg. Chem.* **2004**, *43*, 2427–2434. (z) Habib, M.; Karmakar, T. K.; Aromí, G.; Ribas-Ariño, J.; Fun, H.-K.; Chantrapromma, S.; Chandra, S. K. *Inorg. Chem.* **2008**, *47*, 4109–4117. (z1) Feng, P. L.; Stephenson, C. J.; Amjad, A.; Ogawa, G.; del Barco, E.; Hendrickson, D. N. *Inorg. Chem.* **2010**, *49*, 1304–1306.

(5) (a) Feller, M. C.; Robson, R. *Aust. J. Chem.* **1968**, *21*, 2919. (b) Basu, A.; Kasar, T. G.; Sapre, N. Y. *Inorg. Chem.* **1998**, *27*, 4539–4542. (c) Basu, A.; Saple, A. R.; Sapre, N. Y. *J. Chem. Soc., Dalton Trans.* **1987**, 1797–1799. (d) Sommerer, O. S.; Baker, J. D.; Jensen, W. P.; Hamzan, A.; Jacobson, R. A. *Inorg. Chim. Acta* **1993**, *210*, 173–176. (e) Sommerer, O. S.; Jensen, W. P.; Jacobson, R. A. *Inorg. Chim. Acta* **1990**, *172*, 3–11. (f) Alonzo, G.; Bertazzi, N.; Maggio, F.; Benetollo, F.; Bombieri, G. *Polyhedron* **1996**, *15*, 4269–4273. (g) Wang, S. L.; Richardson, J. W.; Brigg, S. J.; Jacobson, R. A.; Jensen, W. P. *Inorg. Chim. Acta* **1986**, *111*, 67–72. (h) Kavounis, C. A.; Tsiamis, C.; Cardin, C. J.; Zubavichus, Y. *Polyhedron* **1996**, *15*, 385–390. (i) Tangoulis, V.; Raptopoulou, C. P.; Terzis, A.; Paschalidou, S.; Perlepes, S. P.; Bakalbassis, E. G. *Inorg. Chem.* **1997**, *36*, 3996. (j) Tangoulis, V.; Raptopoulou, C. P.; Paschalidou, S.; Tsohos, A. E.; Bakalbassis, E. G.; Terzis, A.; Perlepes, S. P. *Inorg. Chem.* **1997**, *36*, 5270. (k) Tsohos, A. E.; Dyonyssopoulou, S.; Raptopoulou, C. P.; Terzis, A.; Bakalbassis, E. G.; Perlepes, S. P. *Angew. Chem., Int. Ed.* **1999**, *38*, 983. (l) Papaefstathiou, G. S.; Escuer, A.; Raptopoulou, C. P.; Terzis, A.; Perlepes, S. P.; Vicente, R. *Eur. J. Inorg. Chem.* **2001**, 1567–1574. (m) Jedner, S. B.; Schowöpe, H.; Nimir, H.; Rompel, A.; Brown, D. A.; Krebs, B. *Inorg. Chim. Acta* **2002**, *340*, 181–186. (n) Papaefstathiou, G. S.; Escuer, A.; Mautner, F. A.; Raptopoulou, C. P.; Terzis, A.; Perlepes, S. P.; Vicente, R. *Eur. J. Inorg. Chem.* **2005**, 879–893. (o) Efthymiou, C. G.; Raptopoulou, C. P.; Terzis, A.; Boca, R.; Korabic, M.; Mrozinski, J.; Perlepes, S. P.; Bakalbassis, E. G. *Eur. J. Inorg. Chem.* **2006**, 2236–2252. (p) Stamatatos, T. C.; Efthymiou, C. G.; Stoumpos, C. C.; Perlepes, S. P. *Eur. J. Inorg. Chem.* **2009**, 3361–3391 and references cited therein.

(6) (a) Serna, Z. E.; Barandika, M. G.; Cortés, R.; Urtiaga, M. K.; Arriortua, M. I. *Polyhedron* **1999**, *18*, 249–255. (b) Serna, Z. E.; Lezama, L.; Urtiaga, M. K.; Arriortua, M. I.; Barandika, M. G.; Cortés, R.; Rojo, T. *Angew. Chem., Int. Ed.* **2000**, *39*, 344–347. (c) Serna, Z. E.; Barandika, M. G.; Cortés, R.; Urtiaga, M. K.; Barberis, G. E.; Rojo, T. *J. Chem. Soc., Dalton Trans.* **2000**, 29–34. (d) Serna, Z. E.; Cortés, R.; Urtiaga, M. K.; Barandika, M. G.; Lezama, L.; Arriortua, M. I.; Rojo, T. *Eur. J. Inorg. Chem.* **2001**, 865–872. (e) Serna, Z. E. Ph. D. Thesis, UPV/EHU, 2001. (f) Barandika, M. G.; Serna, Z. E.; Cortés, R.; Lezama, L.; Urtiaga, M. K.; Arriortua, M. I.; Rojo, T. *Chem. Commun.* **2001**, 45–46. (g) Serna, Z. E.; Urtiaga, M. K.; Barandika, M. G.; Cortés, R.; Martin, S.; Lezama, L.; Arriortua, M. I.; Rojo, T. *Inorg. Chem.* **2001**, *40*, 4550–4555.

Experimental Section

Materials. All solvents and starting materials for synthesis were purchased commercially and were used as received. Metal(II) nitrate hydrates (Aldrich), the dpk ligand (Lancaster), potassium cyanate, and sodium azidure (Aldrich) were used without further purification.

Synthesis. ***Warning!*** *Azido and perchlorate complexes of metal ions are potentially explosive. Only a small amount of material should be prepared, and it should be handled with caution.*

Synthesis of $[Ni_2(dpk\cdot OH)(dpk\cdot CH_3O)(N_3)(H_2O)]_2(ClO_4)_2\cdot 2H_2O$ (1). This compound was synthesized by the slow addition of a methanolic solution (25 cm^3) containing the dpk ligand (1 mmol) to an aqueous/methanolic solution (25 cm^3) prepared by mixing $Ni(ClO_4)_2\cdot 6H_2O$ (1 mmol) and NaN_3 (1 mmol). The reaction was carried out under continuous stirring at 45 °C. After several days, green prismatic crystals appeared from the resulting solution, which was left standing at room temperature. Yield: 62% (based on nickel). Anal. Calcd for $C_{23}H_{24}N_7O_{10}ClNi_2$: C, 38.8; H, 3.4; N, 13.8. Found: C, 38.2; H, 3.3; N, 14.1. IR (cm^{-1}): 2200 [$\nu_{as}(N_3)$], 1328 [$\nu_s(N_3)$], 1610 [ν(CO)], 1540 (pyridyl stretching), 1020 (pyridyl breathing), 757 (pyridyl C$-$H), 3450 (H_2O_{cryst}), 1100 [$\nu_3(ClO_4)$], 630 [$\nu_4(ClO_4)$]. UV$-$vis (cm^{-1}): 9520 (ν_1), 15380 (ν_2), 25000 (ν_3) from $^3A_{2g}$ to $^3T_{2g}$, $^3T_{1g}$(F), and $^3T_{1g}$(P), respectively. D_q = 952 cm^{-1}, B = 788 cm^{-1}, and C = 2729 cm^{-1}.

Synthesis of $[Ni_2(dpk\cdot OH)(dpk\cdot CH_3O)(NCO)(H_2O)]_2(ClO_4)_2\cdot 2H_2O$ (2). This compound was synthesized by the same method as that for **1**, with the difference of the addition of KNCO (1 mmol) in place of NaN_3. As for **1**, green prismatic crystals were also obtained for **2**. Yield: 55% (based on nickel). Anal. Calcd for $C_{24}H_{24}N_5O_{11}ClNi_2$: C, 40.5; H, 3.4; N, 9.8. Found: C, 39.9; H, 3.5; N, 9.7. IR (cm^{-1}): 2179 [cyanate, ν(C$-$N)], 1604 [ν(CO)], 1444 (pyridyl stretching), 1066 (pyridyl breathing), 763 (pyridyl C$-$H), 3500 (H_2O_{cryst}), 1092 [$\nu_3(ClO_4)$], 684 [$\nu_4(ClO_4)$]. UV$-$vis (cm^{-1}): 9400 (ν_1), 15000 (ν_2), 25000 (ν_3) from $^3A_{2g}$ to $^3T_{2g}$, $^3T_{1g}$(F), and $^3T_{1g}$(P), respectively. D_q = 940 cm^{-1}, B = 787 cm^{-1}, and C = 3197 cm^{-1}.

Synthesis of $[Ni_2(dpk\cdot OH)(dpk\cdot CH_3O)(NCO)(H_2O)]_2(NO_3)_2\cdot 2H_2O$ (3). This compound was synthesized according to the same procedure as that of **1** but using $Ni(NO_3)_2\cdot 6H_2O$ (1 mmol) instead of $Ni(ClO_4)_2\cdot 6H_2O$. Green prismatic crystals were also obtained in this case. Yield: 59% (based on nickel); Anal. Calcd for $C_{24}H_{24}N_6O_{10}Ni_2$: C, 42.8; H, 3.6; N, 12.5. Found: C, 41.9; H, 3.6; N, 12.4. IR (cm^{-1}): 2179 [cyanate, ν(C$-$N)], 1605 [ν(CO)], 1421 (pyridyl stretching), 1068 (pyridyl breathing), 760 (pyridyl C$-$H), 3470 (H_2O_{cryst}), 1384 [$\nu_3(NO_3)$], 684 [$\nu_4(NO_3)$]. UV$-$vis (cm^{-1}): 9351 (ν_1), 15780 (ν_2), 25640 (ν_3) from $^3A_{2g}$ to $^3T_{2g}$, $^3T_{1g}$(F), and $^3T_{1g}$(P), respectively. D_q = 935 cm^{-1}, B = 889 cm^{-1}, and C = 3192 cm^{-1}.

Synthesis of $[Ni_4(dpk\cdot OH)_3(dpk\cdot CH_3O)_2(NCO)](BF_4)_2\cdot 3H_2O$ (4). The synthesis of compound **4** was carried out in a diffusive cell with three compartments. The wing compartments contained (right) an aqueous solution of $NiCl_2\cdot 6H_2O$ (0.5 mmol) and $NaBF_4$ (0.5 mmol) and (left) a methanolic solution of dpk (0.25 mmol) and KNCO (0.5 mmol), while the central one contained a mixture of methanol and water (1:1). After several days, prismatic, green, X-ray-quality single crystals were obtained in the central compartment (< 12% yield based on Ni). Anal. Calcd for $C_{58}H_{55}N_{11}O_{14}B_2F_8Ni_4$: C, 45.3; H, 3.6; N, 10.0. Found: C, 45.0; H, 3.6; N, 10.1. IR (cm^{-1}): 2179 [cyanate, ν(C$-$N)], 1604 [ν(CO)], 1442 (pyridyl stretching), 1035 (pyridyl breathing), 767 (pyridyl C$-$H), 3500 (H_2O_{cryst}), 1045 [$\nu_3(BF_4)$], 684 [$\nu_4(BF_4)$].

Physical Techniques. Microanalyses were performed with a LECO CHNS-932 analyzer. Analytical measurements were carried out in an ARL 3410 + ICP with Minitorch equipment. IR spectroscopy was performed on a Nicolet 520 FTIR spectrophotometer in the 400$-$4000 cm^{-1} region. Diffuse-reflectance spectra were registered at room temperature on a Cary 2415 spectrometer in the 5000$-$45000 cm^{-1} region. Magnetic susceptibilities of powdered samples were carried out in the temperature range 1.8$-$300 K at values of the magnetic field of 0.1, 1.0, 2.0, and 4.0 T, using a Quantum Design Squid magnetometer, equipped with a helium continuous-flow cryostat. The experimental susceptibilities were corrected for diamagnetism of the constituent atoms (Pascal tables). Magnetization of powdered samples was measured at the temperatures of 2 and 5 K.

Table 1. Crystal Data and Structure Refinement for **4**

formula	$Ni_4C_{58}H_{53}N_{11}O_{14}B_2F_8$
M_r	1536.50
cryst syst	monoclinic
space group	$P2_1/c$
a [Å]	14.108(3)
b [Å]	18.190(4)
c [Å]	25.924(7)
β [deg]	105.26(3)
V [Å^3]	6418(3)
Z	4
ρ_{calcd} [g cm^{-3}]	1.590
μ(Mo Kα) [mm^{-1}]	1.251
F(000)	3136
T [K]	293(2)
λ(Mo Kα) [Å]	0.710 69
reflns collected	22 579
unique data measd	11 823
obsd data with I $\geq 2.5\sigma(I)$	11 823
no. of param refined	880
R1[a]	0.0507
wR2[b]	0.1186

[a] $R(F_o) = (\sum||F_o| - |F_c|(\sum|F_o|$. [b] $wR2(F_o^2) = [\sum[w(F_o^2 - F_c^2)^2]/\sum[w(F_o^2)^2]]^{1/2}$.

Crystal Structure Determination. Single-crystal X-ray measurements for compound **1** were taken at room temperature on an Enraf-Nonius CAD-4 diffractometer; full data can be consulted in ref [6b]. Single-crystal X-ray measurements for compound **4** were taken at room temperature on a STOE IPDS I (Imaging Plate Diffraction System) diffractometer with graphite-monochromated Mo Kα radiation (λ = 0.710 73 Å). Corrections for Lorentz and polarization factors were applied to the intensity values. The structures were solved by heavy-atom Patterson methods using the program *SHELXS97*[7] and refined by a full-matrix least-squares procedure on F^2 using *SHELXL97.*[8] Non-H atomic scattering factors were taken from *International Tables of X-ray Crystallography*.[9a] The displacement parameters for the atoms B1 and B2 could not be refined anisotropically. H atoms bonded to C atoms were refined using a riding model with C$-$H = 0.93 Å and U_{iso}(H) = 1.5U_{eq}(C). H atoms bonded to O1w were located in a difference Fourier map, whereas H atoms bonded to O2w were calculated with the program *HYDROGEN*.[9b] Water molecules were tightly restrained to the geometry used in *HYDROGEN* [O$-$H = 0.85(1) Å and H$-$O$-$H = 107(3)°]. H atoms bonded to the highly disordered O3w atom could not be assigned. Interatomic distances involving B and F atoms were restrained to be 1.295(5) Å. Also, the distances O3w···F6 and O3w···F3 were forced to be equal (within 0.02). Antibumping restraints were applied to the closest distances H60$-$(H11w,H21w). In Table 1, crystallographic data and processing parameters for compound **4** are shown. Those corresponding to compound **1** were included in ref [6b].

Powder X-ray Diffraction Data. In the case of compounds **2** and **3**, these data were collected on a Philips X′PERT powder diffractometer with Cu Kα radiation in steps of 0.02° (2θ) over

---

(7) Sheldrick, G. M. *SHELXS97. Program for the Solution of Crystal Structures*; University of Göttingen: Göttingen, Germany, 1997.

(8) Sheldrick, G. M. *Acta Crystallogr.* **2008**, *A64*, 112.

(9) (a) *International Tables for X-ray Crystallography*; Kynoch Press: Birmingham, U.K., 1974; Vol. *IV*. (b) Nardelli, M. *J. Appl. Crystallogr.* **1999**, *32*, 563–571.

the 5−60° (2θ) angular range and a fixed-time counting of 4 s at 25 °C. The powder diffraction patterns were indexed with the program *FULLPROF*[10] based on the Rietveld method[11,12] using the *Profile Matching* option (the lattice parameters of compound **1** were used). Crystallographic data and processing parameters for compounds **2** and **3** are given in Table 2.

Results and Discussion

Structural Analysis for 1−3. Figure 1 displays the X-ray diffraction pattern analyses carried out on the powdered samples for **2** and **3**. They have been fit using the lattice parameters of **1** (see ref [6b]).

The results clearly show that compounds **1**−**3** are isostructural. Thus, the difference between **1** and **2** is the presence of cyanate groups for **2** instead of the azide ligands present for **1**. For **3**, nitrate counteranions should be sited in place of the perchlorate groups present for **1** and **2**.

Compounds **1**−**3** consist of centrosymmetric tetrameric cations (Figure 2) in which the $\mathrm{Ni^{II}}$ ions are connected through μ-1,1-N_3 (**1**) or μ-1,1-NCO (**2** and **3**) and μ-O bridges. Additionally, two ClO_4^- (**1** and **2**) or NO_3^- (**3**) counteranions and two crystallization molecules of water are present per tetrameric unit. A complete description for **1** is detailed in ref [6b]. Each cluster exhibits two end-on pseudohalides (coordinated by N5 and N5i atoms, respectively), two molecules of water (linked through OW1 and OW1i, respectively), two dpk·OCH_3 ligands (chelated by N1, O1, N2 and N1i, O1i, N2i, respectively), and two dpk·OH ligands (chelated by N3, O3, N4 and N3i, O3i, N4i, respectively). Obviously, dpk·OCH_3 and dpk·OH anionic ligands are the result of solvolysis with water and methanol, respectively, followed by an ulterior deprotonation of the original dpk ligands (Scheme 1).

The tetrameric unit in the compounds exhibits a dicubane-like core with two missing vertexes (Figure 3) in which two types of octahedrally coordinated Ni atoms, Ni1 and Ni2, can be distinguished. Thus, the crystallographically related Ni2 and Ni2i occupy two vertexes of the common face of the dicubane unit, with both metallic atoms being doubly O-bridged through O3 and O3i atoms (sited on the other two vertexes and belonging to dpk·OH). These O atoms act as triple bridges because they are also bonded to N1 and N1i atoms, respectively, along the edges of both cubic subunits. Atom Ni1 is also doubly bridged to Ni2, through O1 (dpk·OCH_3), and to Ni2i, through N5 (end-on pseudohalide). Obviously, Ni1i is symmetrically bonded to Ni2 and Ni2i. Table 3 summarizes some selected structural parameters for **1**.

Table 2. Crystallographic Data for **2** and **3**

	2	**3**
formula	$Ni_2C_{24}H_{24}N_5ClO_{11}$	$Ni_2C_{24}H_{24}N_6O_{10}$
M_w	1422.68	1347.78
space group	$P2_1/c$	$P2_1/c$
a [Å]	13.443(2)	13.289(2)
b [Å]	11.008(1)	10.972(2)
c [Å]	19.910(2)	20.007(3)
β [deg]	91.553(9)	91.07(2)
V [Å^3]	2945(3)	2916(6)
Z	2	2
T [K]	293	293
λ(Mo Kα) [Å]	1.54	1.54
R_b[a]	3.77	3.74
R_p[b]	6.17	9.79
R_{wp}[c]	8.26	12.4
GOF[d]	7.44	4.13

[a] $R_b = 100[\sum|I_o - I_c|]/\sum|I_o|$. [b] $R_p = 100[\sum|y_o - y_c|]/\sum|y_o|$. [c] $R_{wp} = [\sum[w|y_o - y_c|^2]/\sum[w|y_o|^2]]^{1/2}$. [d] GOF = $[R_{wp}/R_{expected}]^2$.

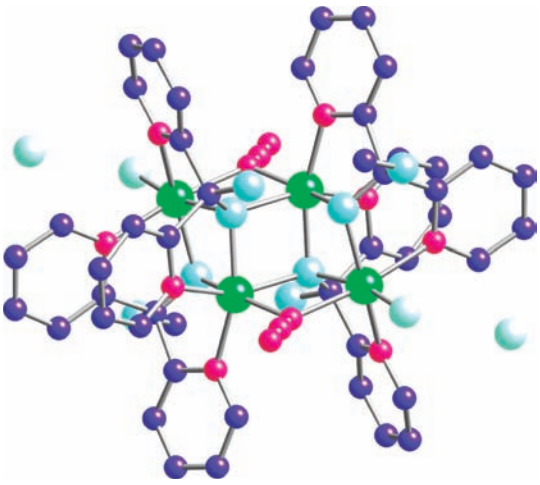

Figure 2. Crystal structure, of the corresponding cationic sections, for compounds **1**−**3**.

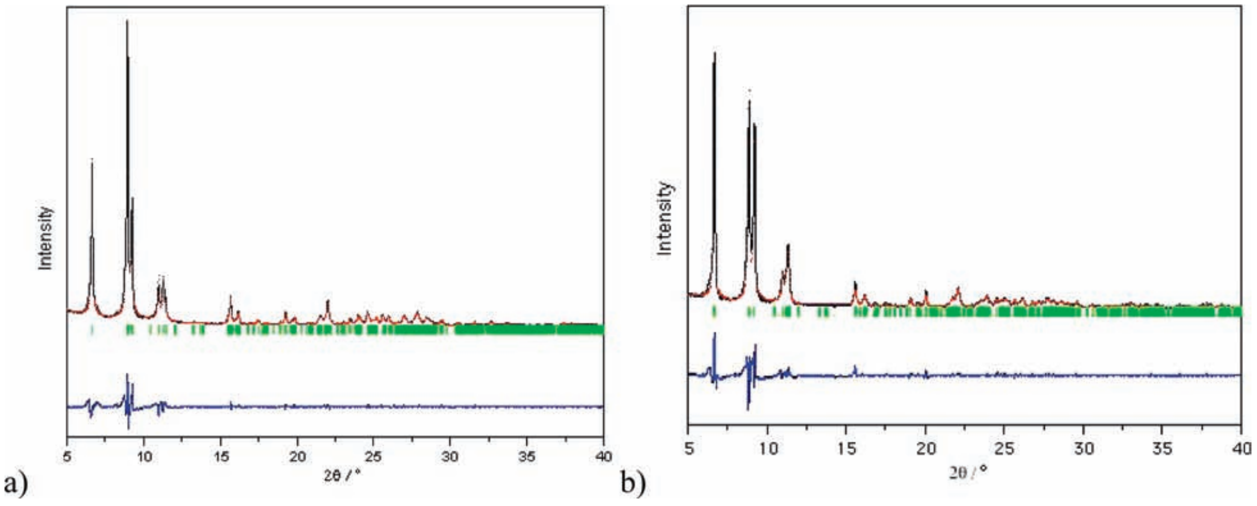

Figure 1. X-ray diffraction pattern analysis for (a) **2** and (b) **3**.

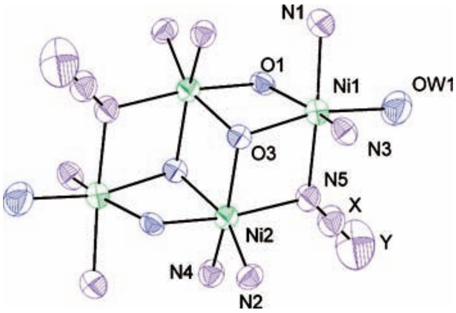

Figure 3. Dicubane unit scheme for compounds **1**−**3** (X = N or C; Y = N or O).

Table 3. Selected Bond Lengths [Å] and Angles [deg] for **1**[a]

Ni1−O1	2.032(5)	Ni2−N5−Ni1i	101.8(3)
Ni1−OW1	2.095(6)	O3−Ni2−O3i	80.8(2)
Ni1−N3	2.085(6)	N2−Ni2−O3i	107.0(2)
Ni1−N1	2.086(7)	N5−Ni2−O3i	78.9(2)
Ni1−N5i	2.110(7)	N4−Ni2−O3i	154.3(2)
Ni1−O3	2.124(5)	N2−Ni2−O1	77.6(2)
Ni2−O3	2.014(5)	N5−Ni2−O1	163.1(2)
Ni2−N2	2.024(6)	O3i−Ni2−O1	87.0(2)
Ni2−N5	2.076(6)	O1−Ni1−N3	156.9(2)
Ni2−N4	2.083(7)	O1−Ni1−OW1	101.4(2)
Ni2−O3i	2.098(5)	N3−Ni1−OW1	100.4(3)
Ni2−O1	2.120(5)	N3−Ni1−N1	95.2(3)
N5−N6	1.186(9)	OW1−Ni1−N1	88.6(3)
N6−N7	1.137(11)	O1−Ni1−N5i	92.6(2)
Cl−O8	1.33(3)	N3−Ni1−N5i	95.2(3)
Cl−O5	1.37(2)	OW1−Ni1−N5i	89.5(3)
Cl−O6	1.55(2)	N1−Ni1−N5i	169.6(3)
		O1−Ni1−O3	83.1(2)
		N7−N6−N5	176.7(10)

[a] Symmetry code: i, −*x*, −*y*, −*z*.

Description of the Structure for 4. Compound **4** also exhibits a tetrameric defective dicubane unit as the central core (Figure 4). However, in this case, the tetramer is not centrosymmetric. Thus, one cyanate ligand, three dpk·OH, and two dpk·$\mathrm{OCH_3}$ groups act as bridges providing μ-1,1-NCO and μ-O links. As observed in Figure 5, the five dpk·OR ligands perform as N,O,N′-tridentated: N1−O1−N2, N3−O3−N4, and N5−O5−N6 are the linking atoms for the three dpk·OH groups, while the sets N7−O7−N8 and N9−O9−N10 correspond to the two dpk·$\mathrm{OCH_3}$ groups. The cyanate group is bonded by the N11 atom.

The four Ni atoms in the tetramer are octahedrally coordinated. The Ni2 and Ni4 atoms, located on the common face of the dicubane unit, are linked through the O3 and O5 atoms. These atoms perform as μ_3-O links, being also bonded to Ni1 and Ni3, respectively. The latter Ni atoms are doubly connected to the common face. Thus, Ni1 is also linked to Ni2 and Ni4 through O1 and N11, respectively, while Ni3 connects with Ni4 through O9 and with Ni2 through O7. Therefore, O1, O7, O9, and N11 perform as μ_2-links.

Table 4 displays some selected bond distances (Å) and angles (deg) for **4**. The $\mathrm{Ni{-}N_{cyanate}}$ average distance is 2.084(4) Å, while the $\mathrm{Ni{-}N_{cyanate}{-}Ni}$ angle is 97.5(2)°. On the other hand, the average distances between Ni and μ_2-O and μ_3-O atoms are very similar: 2.060(3) and 2.077(3) Å, respectively. The Ni−O−Ni angles range from 93.2(2) to 104.4 (2)°, while the Ni···Ni distances range from 3.030 to 3.228 Å. Finally, on average, the B−F distance and F−B−F angle are 1.31(3) Å and 110(5)°, respectively.

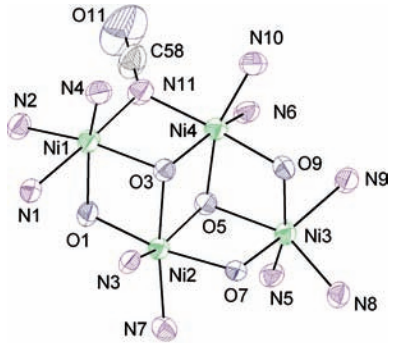

Figure 4. ORTEP view (50% probability level) of the dicubane unit for **4**.

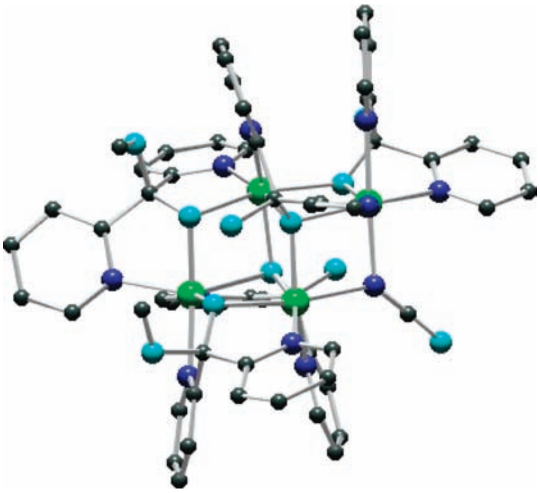

Figure 5. Complete structure of the complex cation for **4**.

Dicubane Unit. Coordination tetramers have been observed to adopt several structures like cubanes,[3g,13] square[3h,14] and lineal[15] entities, butterfly cores,[16] and dicubanes with the missing vertexes[17] (Scheme 2). The dicubanes found in the literature are centrosymmetric, exhibiting very similar values of the bond distances and angles (Table 5). Among the dicubanes, the singularity of compounds **1**−**4** lies in the presence of pseudohalides performing as intermetallic bridges.

---

(10) Rodriguez-Carvajal, J. *FULLPROF: A Program for Rietveld Refinement and Pattern Matching Analysis*; Abstracts of the Satellite Meeting on Powder Diffraction of the XV Congress of the IUCr; IUCr: Toulouse, France, 1990; p 127.

(11) Rietveld, H. M. *Acta Crystallogr.* **1967**, *12*, 151–152.

(12) Rietveld, H. M. *J. Appl. Crystallogr.* **1969**, *6*, 65–67.

(13) (a) Ballester, L.; Coronado, E.; Gutiérrez, A.; Monge, A.; Perpiñan, M. F.; Pinilla, E.; Rico, T. *Inorg. Chem.* **1992**, *31*, 2053. (b) Kortz, U.; Terzé, A.; Hervé, G. *Inorg. Chem.* **1999**, *38*, 2038.

(14) (a) Wang, S.; Trepanier, S. J.; Zheng, J.-C.; Peng, Z.; Wagner, M. J. *Inorg. Chem.* **1992**, *31*, 2118. (b) Teipel, S.; Griesar, K.; Haase, W.; Krebs, B. *Inorg. Chem.* **1994**, *33*, 456.

(15) (a) Blondin, G.; Davydov, R.; Philouze, C.; Charlot, M.-F.; Styring, S.; Åkemark, B.; Girerd, J.-J.; Boussac, A. *J. Chem. Soc., Dalton Trans.* **1997**, 4069. (b) Papadopoulos, A. N.; Tangoulis, V.; Raptopoulou, C. P.; Terzis, A.; Kessissoglou, D. P. *Inorg. Chem.* **1996**, *35*, 559.

(16) (a) Castro, S. L.; Sun, Z.; Grant, C. M.; Bollinger, J. C.; Hendrickson, D. N.; Christou, G. *J. Am. Chem. Soc.* **1998**, *120*, 2365. (b) Wemple, M. W.; Coggin, D. K.; Vincent, J. B.; McCuster, J. K.; Streib, W. E.; Huffman, J. C.; Hendrickson, D. N.; Christou, G. *J. Chem. Soc., Dalton Trans.* **1998**, 719.

This kind of structural disposition for a tetramer is not very common, as illustrated by the fact that a scarce number of nickel tetramers of this type have been reported so far.[3b,j,5m,5o,6c,17d]

The trend of the dpk derivatives to chelate as N,O,N′-terdentate could be interpreted in terms of enhancing of the generation of intermetallic links. On the other hand, among the different possibilities for tetrameric topologies, the dicubane and cubane types exhibit remarkably high connectivity between metallic centers. Thus, for octahedral cations, both the dicubane and cubane just exhibit 16 coordination positions. However, the dicubane seems to be more appropriate for the voluminous organic ligands. In fact, as illustrated by **4**, up to five dpk derivatives can be accommodated in this way.

The idea that the adoption of the dicubane-like structure for **1**−**4** is related to the coordination performance of dpk is reinforced by the fact that variations of neither the pseudohalide nor the counteranion imply significant changes on the general structural disposition. Moreover, compounds **1**−**3** are isomorphous. As mentioned above, compound **4** does not follow the same pattern of structural disposition even if, with the exception of the counteranion, compounds **2** and **4** exhibit the same components. Thus, a comparison between counteranions BF_4^- (present in **4**) and ClO_4^- (present in **2**) does not suggest any significant differences in the size and morphology as to justify the adoption of a different structure. At this point, it must be pointed out that the attempts made to obtain a Ni-dpk-NCO-BF_4 pure product according to the procedure for **1**−**3** were completely unfruitful (compounds **1**−**3** were obtained from a one-pot reaction). Therefore, a diffusive-cell synthesis procedure was followed to obtain compound **4**.

Table 4. Selected Bond Lengths [Å] and Angles [deg] for **4**

Ni1−N4	2.049(4)	Ni1−O1	2.064(3)
Ni1−O3	2.064(3)	Ni1−N2	2.074(4)
Ni1−N11	2.101(4)	Ni1−N1	2.164(4)
Ni2−O7	2.005(3)	Ni2−O3	2.059(3)
Ni2−N3	2.090(4)	Ni2−N7	2.095(4)
Ni2−O1	2.129(4)	Ni2−O5	2.152(3)
Ni3−O7	2.028(3)	Ni3−O9	2.032(3)
Ni3−N8	2.076(4)	Ni3−N9	2.109(4)
Ni3−N5	2.113(4)	Ni3−O5	2.136(3)
Ni4−O5	2.031(3)	Ni4−N10	2.045(4)
Ni4−N11	2.087(4)	Ni4−N6	2.088(4)
Ni4−O3	2.097(3)	Ni4−O9	2.116(4)
N11−C58	1.177(7)	C58−O11	1.177(7)
B1−F2	1.297(5)	B1−F3	1.297(5)
B1−F1	1.297(5)	B1−F4	1.309(5)
B2−F5	1.311(5)	B2−F8	1.312(5)
B2−F6	1.309(5)	B2−F7	1.310(5)
N4−Ni1−O1	156.49(15)	N4−Ni1−O3	79.18(16)
O1−Ni1−O3	84.63(13)	N4−Ni1−N2	117.27(18)
O1−Ni1−N2	80.45(16)	O3−Ni1−N2	163.29(15)
N4−Ni1−N11	94.68(17)	O1−Ni1−N11	99.95(15)
O3−Ni1−N11	82.28(15)	N2−Ni1−N11	92.89(17)
N4−Ni1−N1	87.47(16)	O1−Ni1−N1	79.09(14)
O3−Ni1−N1	101.39(14)	N2−Ni1−N1	83.18(17)
N11−Ni1−N1	176.06(17)	O7−Ni2−O3	94.23(13)
O7−Ni2−N3	91.28(15)	O3−Ni2−N3	77.69(14)
O7−Ni2−N7	78.70(16)	O3−Ni2−N7	172.47(16)

Table 5. Connectivity Parameters (Distances in Å and Angles in deg) for Dicubane-Like Tetramers, According to Scheme 3

cation	*d*(1−2)	*d*(1−2i)	*d*(2−2i)	*d*(1−1i)	ref
Cu^{II}[a]	3.121	2.954	3.230	5.458	17a
Mn^{II,III}[b]	3.211	3.112	2.744	5.846	17b
Fe^{III}[c]	3.212	3.230	3.214	5.772	17c
Mn^{II}[d]	3.370	3.394	3.323	5.893	6e
Co^{II}[e]	3.144	3.283	3.291	5.712	6f
Ni^{II}[f]	3.063	3.238	3.145	5.463	6c
Ni^{II}[g]	3.124	3.109	3.196	5.352	3b
Ni^{II}[h]	3.096	3.210	3.152	5.444	17d
Ni^{II}[I]	3.075	3.279	3.152	5.520	5m
Ni^{II}[j]	3.107	3.131	3.163	5.385	5m
Ni^{II}[k]	3.089	3.273	3.178	5.515	5o
Ni^{II}[l]	3.079	3.135	3.135	5.504	3j
Ni^{II}[m]	3.054	3.248	3.133	5.472	this work
Ni^{II}[n]	3.030	3.140	3.228	5.309	this work
	3.075	3.185			

[a] $[Cu_4(tde)_2(hfacac)_4]$ (H_2tde = 2,2′-thiodiethanol; Hhfacac = 1,1,1,5,5,5-hexafluoroacetylacetonate). [b] $[Mn_2(MeOH)L(OH)(bpy)]_2$. [c] $[Fe_4(MeO)_2(acac)_4(N_3)_2]$. [d] $[Mn_2(dpk\cdot OH)(dpk\cdot OCH_3)(N_3)_2]_2$. [e] $[Co_2(dpk\cdot OH)(dpk\cdot OCH_3)(NCO)_2]_2$. [f] $[Ni_4(dpk\cdot OH)_4(N_3)_4]$. [g] $[Ni_4(H_2O)_2(PW_9O_{34})_2]^{10-}$. [h] $[Ni_4(H_2L)_2(OCH_3)_2(CH_3CO_2)_2(N_3)_2]$. [I] $[Ni_4(dpk\cdot OH)_4(CH_3COO)_4]\cdot 4CH_3CH_2OH$. [j] $[Ni_4(dpk\cdot OH)_2(dpk\cdot OCH_2CH_3)_2(CH_3CONHO)_2]Cl_2$. [k] $[Ni_4(O_2CMe)_4[(2\text{-py})_2C(OH)O]_4]\cdot 2MeCN$. [l] $[Ni_2(dpk\cdot (O)(OH)(dpk\cdot (O)(OCH_3)(N_3)_2]_2$. [m] Compound **1**. [n] Compound **4** (noncentrosymmetric).

Scheme 3. Structural Parameters for This Type of Defective Dicubane

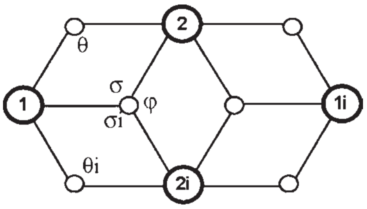

Scheme 2. Known Structures for Coordination Tetramers

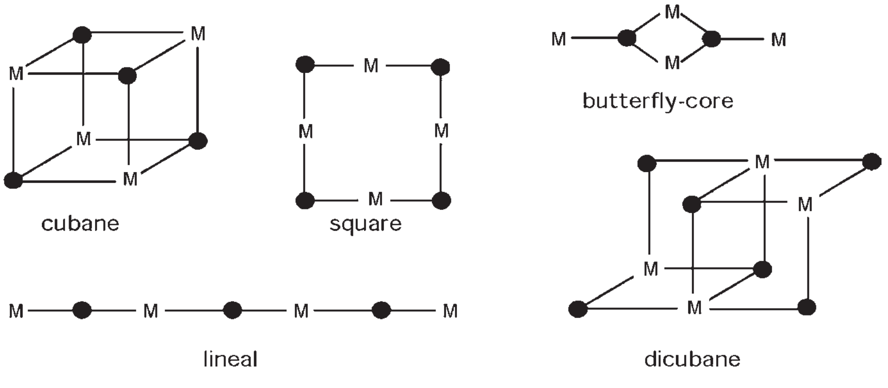

Taking into account that dicubane-like cores have also been reported for Cu^{II},[17a] $Mn^{II,III}$,[17b] and Fe^{III} [17c] systems, the convenience of studying other dpk-metallic systems with pseudohalides seems to be clear. Particularly, the relationship between the dicubanes and the use of the dpk organic ligand should be clarified in order to rationalize the adoption of a determined structure. In this sense, it could be mentioned that our results confirm that Co^{II} [6f] and Mn^{II} [6e,51] tetrameric systems also exhibit the defective dicubane structure.

Magnetic Measurements and Coupling Constants Calculation. Susceptibility measurements were performed between 2 and 300 K for compounds **1**−**4**. Figure 6 shows the thermal variation of $\chi_m T$ at a 1000 G magnetic field for **1**−**4**. The curve for **2** is nearly identical with the one for **3**. As observed in Figure 6, the $\chi_m T$ product continuously increases upon cooling, reaching a maximum, after which it tends to 0. The $\chi_m T$ curve goes up from 1.17 (**1**), 1.17 (**2**), 1.18 (**3**), and 1.16 (**4**) $cm^3\ mol^{-1}$ K (per Ni atom) at room temperature, reaching maximum values of 2.61 (**1**), 2.57 (**2**), 2.63 (**3**), and 2.60 (**4**) $cm^3\ mol^{-1}$ K (per Ni atom) between 6 and 10 K, respectively, after which it tends to zero. The Curie−Weiss law is obeyed down to 60 (**1**), 50 (**2**), 40 (**3**), and 50 (**4**) K with values of C_m, θ, and g of 1.15 $cm^3\ mol^{-1}$ K, +31.1 K, and 2.1, respectively, for **1**; 1.21 $cm^3\ mol^{-1}$ K, +25.6 K, and 2.1, respectively, for **2**; 1.25 $cm^3\ mol^{-1}$ K, +20.7 K, and 2.2, respectively, for **3**; and 1.15 $cm^3\ mol^{-1}$ K, +31.1 K, and 2.1, respectively, for **4**.

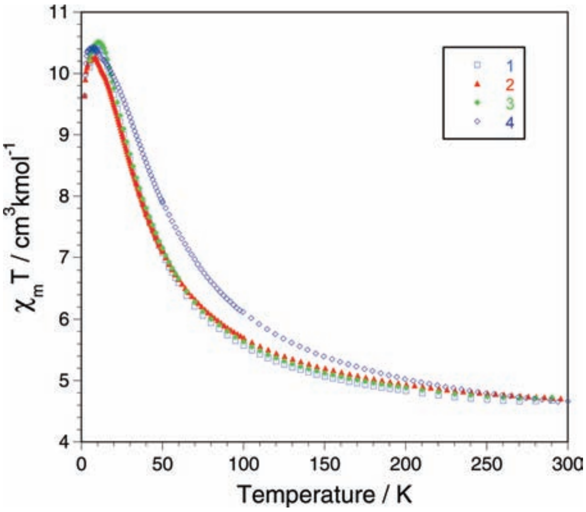

Figure 6. Thermal variation of $\chi_m T$, per four Ni atoms at 1000 G for **1**−**4**.

Susceptibility measurements at different fields (0.1, 1, 2, and 4 T), on polycrystalline samples ground and compacted, have been made for compounds **1** and **4** (see Figure 7). Thermal variations have been made from 2 to 50 K, except for the 1000 G field, where room temperature has been reached. At all of the fields measured, it can be observed as the $\chi_m T$ product increases with decreasing temperature and reaches a maximum between 7 and 20 K as a function of the applied magnetic field, being indicative of the existence of ferromagnetic interactions between the Ni^{II} ions. Below the maximum, $\chi_m T$ decreases rapidly, tending to zero. This fall is a consequence of the splitting of the ferromagnetic ground state ($S = 4$) due to the anisotropy of the isolated ions and to the Zeeman coupling between the spins and the applied external magnetic field. In order to separate these two contributions, susceptibility measurements at different fields have been done.

Considering the structure of the studied systems and the nature of the metal ions, the following Hamiltonian has been chosen to reproduce the experimental magnetic behavior:

$$\hat{H} = -2J_1(\hat{S}_1\hat{S}_3 + \hat{S}_2\hat{S}_4) - 2J_2(\hat{S}_1\hat{S}_4 + \hat{S}_2\hat{S}_4) - 2J_3\hat{S}_1\hat{S}_2 + D(\hat{S}_{Z1}^2 + \hat{S}_{Z2}^2 + \hat{S}_{Z3}^2 + \hat{S}_{Z4}^2)$$

The interaction in the larger diagonal has been considered to be negligible, and D is the anisotropy parameter of the isolated ions for each Ni ion. Intermolecular interactions have also been neglected because the tetramers are isolated and separated by the different counterions.

In order to evaluate the magnetic properties, the *MAGPACK*[18] package of programs has been used. This package allowed us to calculate the energy levels and different

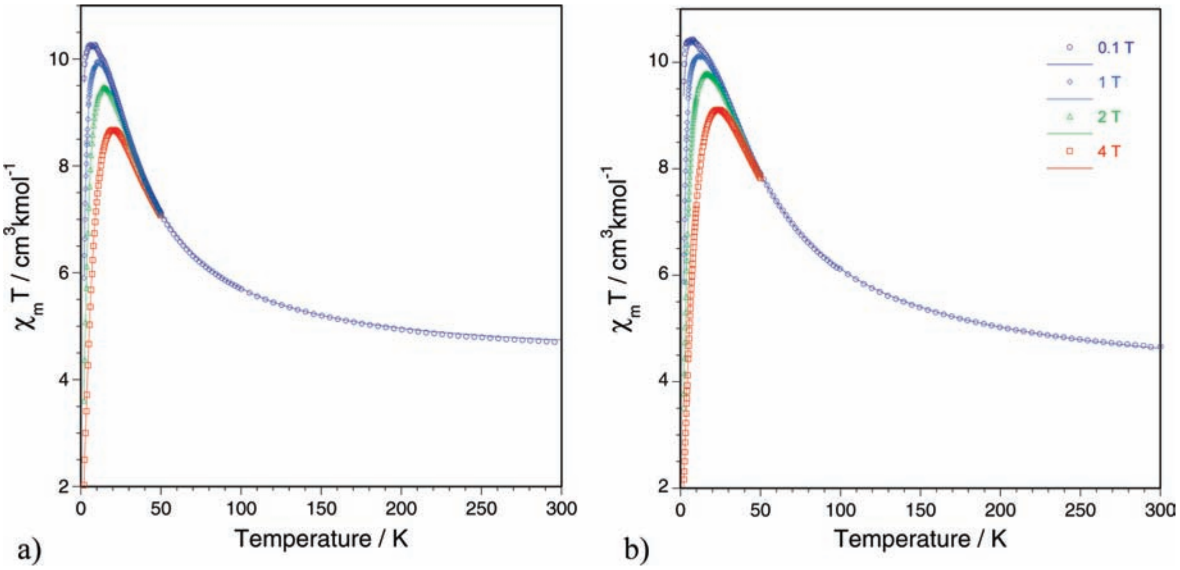

Figure 7. Susceptibility measurements at different magnetic fields for (a) compound **1** and (b) compound **4**.

Scheme 4. Defined Coupling Constants for Dicubanes

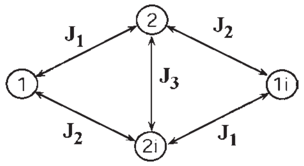

properties considering isotropic and anisotropic exchange interactions between the different magnetic centers. The method used to calculate the energy matrix is based on the irreducible tensor operators (ITO).[19] It uses the spin symmetry of the system and reduces the dimension and the time for the energy matrix diagonalization.

In order to evaluate the susceptibility curves, the Zeeman term has been added to the Hamiltonian

$$\hat{H}_{\mathrm{ZEE}} = \sum_{j=x,y,z}\;\sum_{i=1,2,3,4} \beta g_i^j \hat{S}_i^j H^j$$

Considering that the measurements have been done on polycrystalline samples and that the system shows an important magnetic anisotropy, we must take into account the magnetic field orientation on the magnetic anisotropy axe of this system. In order to do this, we have evaluated the energy levels and their variation with the applied field for different relative orientations of the magnetic field and the molecular anisotropy axe. Evaluated susceptibility will be an average of these different contributions. In this case, the susceptibility for the angles between the anisotropy axe and the external field ranges from 0 to 90° every 10°.

The procedure to fit the susceptibility curve is a simultaneous minimization of the different $\chi_m T$ curves corresponding to different magnetic fields. The best fit is the one that minimizes the function

$$R = \sum_H \sum_i \frac{(\chi T_{\mathrm{exp}} - \chi T_{\mathrm{calc}})^2}{\chi T_{\mathrm{exp}}{}^2}$$

where H corresponds to the different magnetic fields and i the points measured for each field.

Scheme 4 shows the different J values considered. The best set of parameters is $J_1 = J_2 = 5.6\ \mathrm{cm}^{-1}$, $J_3 = 11.8\ \mathrm{cm}^{-1}$, $D = 5.6\ \mathrm{cm}^{-1}$, and $g = 2.03$ ($R = 1.63 \times 10^{-5}$) for **1**; $J_1 = J_2 = 5.5\ \mathrm{cm}^{-1}$, $J_3 = 12.0\ \mathrm{cm}^{-1}$, $D = 5.6\ \mathrm{cm}^{-1}$, and $g = 2.03$ ($R = 5.2 \times 10^{-5}$) for **2**; $J_1 = J_2 = 6.3\ \mathrm{cm}^{-1}$, $J_3 = 4.9\ \mathrm{cm}^{-1}$, $D = 6.2\ \mathrm{cm}^{-1}$, and $g = 2.21$ ($R = 1.9 \times 10^{-5}$) for **3**; $J_1 = J_2 = 7.0\ \mathrm{cm}^{-1}$, $J_3 = 15.0\ \mathrm{cm}^{-1}$, $D = 4.8\ \mathrm{cm}^{-1}$, and $g = 2.06$ ($R = 1.75 \times 10^{-4}$) for **4**. The calculated curves are shown in Figure 7 as continuous lines. Because of the large number of parameters, we have assumed an isotropic g and equal for the four Ni atoms inside every tetramer. Differentiation of J_1 and J_2 for **1**−**3** does not improve the fit. On the contrary, the solution found, if the three parameters were set equal, clearly has a lower quality. In the case of compound **4**, considering that it is noncentrosymmeric, a fit with different J_1 and J_2 gave the following results: $J_1 = 6.9\ \mathrm{cm}^{-1}$, $J_2 = 7.0\ \mathrm{cm}^{-1}$, $J_3 = 15.2\ \mathrm{cm}^{-1}$, $D = 4.8\ \mathrm{cm}^{-1}$, and $g = 2.06$ ($R = 1.62 \times 10^{-5}$). This fit was the one finally used.

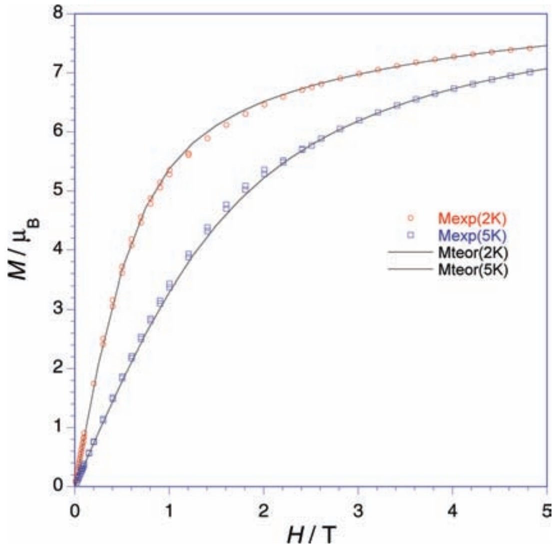

Figure 8. Field dependence of magnetization, at 2 and 5 K, for **4**.

The field dependence of magnetization, M, was also recorded at 2 and 5 K [$0 \le H(T) \le 5$] for **1**−**4**. Figure 8, which shows the results for **4**, is illustrative of the four compounds. As observed, M reaches the saturation value expected for a tetranuclear ferromagnetic nickel(II) compound, i.e., $N\beta g/2$ (≈ 8). Starting from the best set of parameters, the experimental magnetization curves can perfectly be fitted, as can be observed in Figure 8. For this simulation, the same type of integration of the magnetic field orientation and the anisotropy of the system has been performed.

Magnetization curves have also been adjusted using a model with a molecular ground state $S = 4$ (Figure S1 of the Supporting Information). The best fit gives a $D(S=4)$ value of $2.8\ \mathrm{cm}^{-1}$. The quality of this fit is much worse than the fit with the four $S = 1$ spins ferromagnetically coupled. Because the J and D values are of the same order, the ground state is not isolated enough from the excited states (see Figure 9), so its splitting does not follow a simple pattern proportional to $S_Z{}^2$ and D can be overestimated. For more detailed information about this splitting, other measures are necessary that directly provide energy levels such as high-field electron paramagnetic resonance or inelastic neutron scattering.

Strictly, the fit of the susceptibility can be done only at fields where magnetization is linear with the field. At low temperatures (< 5 K), this linear dependence only occurs at fields weaker than 1 T. However, as the temperature increases, so does the range of applicable fields. Therefore, we can see that, in the areas around the maxima of the $\chi_m T$ product and at higher temperatures than these maxima, the linear dependencies are satisfied. Only a few points at lower temperatures and high fields below these maxima do not satisfy this condition, and their contribution may be considered small. Thus, the great majority of the fitting points is optimal and gives a correct exchange and local anisotropy parameters. The validity of the parameters extracted from this procedure can be confirmed by

---

[17] (a) Breeze, S. R.; Wang, S.; Creedan, J. E.; Raju, N. P. *J. Chem. Soc., Dalton Trans.* **1998**, 2327–2334. (b) Sunatsuki, Y.; Shimada, H.; Matsuo, T.; Nakamura, M.; Kai, F.; Matsumoto, N.; Re, N. *Inorg. Chem.* **1998**, *37*, 5566–5574. (c) Li, H.; Zhong, Z. J.; Chen, W.; Tou, X.-Z. *J. Chem. Soc., Dalton Trans.* **1997**, 463–464. (d) Tandon, S. S.; Bunge, S. D.; Rakosi, R.; Xu, Z.; Thompson, L. K. *J. Chem. Soc., Dalton Trans.* **2009**, 6536–6551.

[18] Borrás-Almenar, J. J.; Clemente-Juan, J.-M.; Coronado, E.; Tsukerblat, B. S. *J. Comput. Chem.* **2001**, *22*, 985–991.

[19] Borrás-Almenar, J. J.; Clemente-Juan, J.-M.; Coronado, E.; Tsukerblat, B. S. *Inorg. Chem.* **1999**, *38*, 681–688.

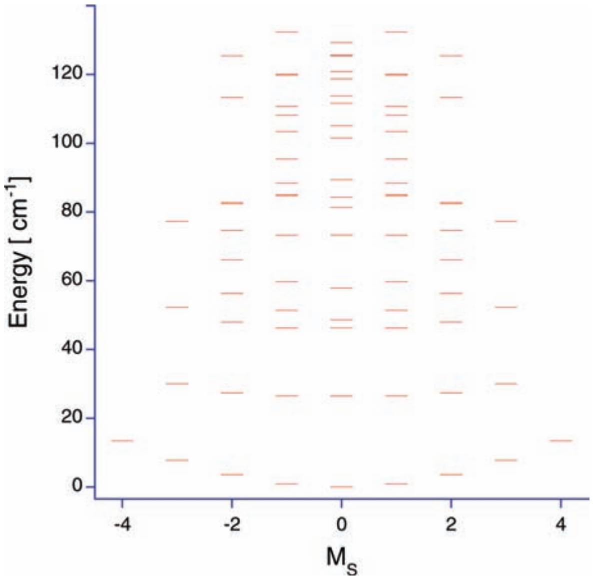

Figure 9. Energy levels as a function of M_s obtained from the best set of parameters of the susceptibility curve fit for compound **4**.

reproducing the magnetization curves (Figure 8) including the area of saturation.

Starting from these parameters, we can also determine the energy levels of the system. In Figure 9, these energy levels are shown as a function of the quantum number M_s. We can see that the ground levels correspond to the $S = 4$ multiplet, split by the anisotropy of the isolated ions. In this ground-state multiplet, we can see, as a function of $M_s = 0$, the ground level, and starting from it, the levels $M_s = \pm1, \pm2, ..., \pm4$ successively appear. This disposition is that expected for a positive sign for D. The same disposition can be observed for the first excited-state multiplet, which corresponds to an $S = 3$. Above this, the different multiplets overlap, giving rise to a very complex level structure.

Conclusion

Using adequate combinations of azide and cyanate pseudohalides together with the dpk ligand and different counterions has led us to the preparation of four new defective dicubane-like nickel(II) tetranuclear compounds. Three of them are isostructural and centrosymmetric (**1**−**3**), while compound **4** is noncentrosymmetric.

Magnetic results indicate that ferromagnetic interactions are taking place for **1**−**4**. The decrease of the magnetic moment observed for all compounds at low temperatures should be attributed to both the characteristic zero-field splitting (ZFS) of the Ni^{II} ion and/or the occurrence of intermolecular interactions. Because the tetranuclear units are isolated by the counteranions in the four compounds, the intermolecular interactions are expected to be negligible.

The magnetic behavior of **1**−**4** can be explained by the existence of end-on azido/cyanato bridges, with angles close to 100°, giving rise to moderately strong ferromagnetic interactions, which are added to the moderate ferromagnetic ones associated with the oxo bridges. Otherwise, the two ferromagnetically coupled μ-azido/μ-cyanato, μ-oxo Ni$_2$ units would couple antiferromagnetically to $S = 0$, irrespective of the relative magnitude of the different J values. Compounds **2**−**4** contain the rarer end-on N-cyanate bridging showing again ferromagnetism.

Table 6. Magnetic Exchange Constant Values, J (cm^{-1}), for Dicubane-Like Tetramers (According to Scheme 4)

cation	J_1	J_2	J_3	ref
Cu^{II} [a]		AF		17a
Mn^{II,III} [b]	−3.5	−3.5	−14.1	17b
Fe^{III} [c]		AF		17c
Mn^{II} [d]		F		6e
Co^{II} [e]		F		6g
Ni^{II} [f]	+6.5	+6.5	+2.5	3b
Ni^{II} [g]	+18.8	+6.9	+1.3	6c
Ni^{II} [h]	−5.3	−4.6	+15.7	5o
Ni^{II} [I]	+7.07	+7.08	+11.4	3j
Ni^{II} [j]	+5.6	+5.6	+11.8	this work
Ni^{II} [k]	+5.5	+5.5	+12.0	this work
Ni^{II} [l]	+6.3	+6.3	+4.9	this work
Ni^{II} [m]	+6.9	+7.0	+15.2	this work

[a] $[Cu_4(tde)_2(hfacac)_4]$ (H_2tde = 2,2′-thiodiethanol; Hhfacac = 1,1,1,5,5,5-hexafluoroacetylacetonate). [b] $[Mn_2(MeOH)L(OH)(bpy)]_2$. [c] $[Fe_4(MeO)_2(acac)_4(N_3)_2]$. [d] $[Mn_4(dpk\cdot OH)_4(N_3)_4]$. [e] $[Co_2(dpk\cdot OH)(dpk\cdot OCH_3)N_3(H_2O)]_2(BF_4)\cdot 4H_2O$. [f] $[Ni_4(H_2O)_2(PW_9O_{34})_2]^{10-}$. [g] $[Ni_4(dpk\cdot OH)_4(N_3)_4]$. [h] $[Ni_4(O_2CMe)_4[(2\text{-}py)_2C(OH)O]_4]\cdot 2MeCN$. [I] $[Ni_2(dpk\cdot(O)(OH)(dpk\cdot(O)(OCH_3)(N_3)_2]_2$. [j] Compound **1**. [k] Compound **2**. [l] Compound **3**. [m] Compound **4** (no centrosymmetric). AF = antiferromagnetic interactions not evaluated. F = ferromagnetic interactions not evaluated.

If we analyze the different magnetic fittings in the case of compound **1**, which we previously published as a communication,[6b] it can be stated that, in the absence of a specific magnetic model for a determined system, the influence of the method employed to fit it is determinant. So, with a 4J approximation, a set of $J_1 = 18.0$, $J_2 = 15.3$, $J_3 = 27.1$, $J_4 = -1.6$ cm^{-1}, and $g = 2.06$ is obtained; with a 2J and D approximation, we obtain $J_A = 14.7$, $J_B = 29.1$ cm^{-1}, $D = -0.068$ cm^{-1}, and $g = 2.12$; in this work, the closest approximation is $J_1 = J_2 = 5.6$, $J_3 = 11.8$ cm^{-1}, $D = 5.6$ cm^{-1}, and $g = 2.03$. Slight differences in the experimental points for compound **1** in this work may be attributed to the specific preparation of the new sample for the measurements performed in this case.

Table 6 summarizes the magnetic exchange constants for other defective dicubanes found in the literature. As observed, tetramers of all of the metal(II) ions, except the copper one, are ferromagnetic. All of the nickel(II) tetramers are ferromagnetic and exhibit moderate values of the J constants. The positive D value calculated for these tetramers precludes a possible behavior as a single-molecule magnet.

Acknowledgment. This work was supported by the Universidad del País Vasco (UPV/EHU; 00169.125-13956/2004), the Spanish Ministerio de Ciencia y Tecnología (MCYT; CTQ2005-05778-PPQ), and the Basque Government (Project IT-282-07). E.C. and J.M.C.-J. are thankful for financial support from the Spanish Ministerio de Ciencia e Innovación, with FEDER cofinancing (Project Consolider-Ingenio in Molecular Nanoscience CSD2007-00010 and Projects MAT2007-61584 and CTQ2008-06720), and the Generalitat Valenciana (PROMETEO Program). N.D.P. thanks UPV/EHU for financial support from "Convocatoria para la concesión de ayudas de especialización para investigadores doctores en la UPV/EHU (2008)".

Supporting Information Available: Crystallographic information, as CIF files, for compounds **1** and **4** and magnetization curves. This material is available free of charge via the Internet at http://pubs.acs.org.